

The effect of Zn^{2+} on the secondary structure of a histidine-rich fusogenic peptide and its interaction with lipid membranes

H. Binder ^{a,*}, K. Arnold ^a, A.S. Ulrich ^b, O. Zschörnig ^a

^a University of Leipzig, Institute of Medical Physics and Biophysics, Liebigstr. 27, D-04103 Leipzig, Germany

^b Friedrich-Schiller-University of Jena, Institute of Molecular Biology, Winzerlaer Str. 10, 07745 Jena, Germany

Received 17 April 2000; accepted 6 July 2000

Abstract

Membrane fusion between uncharged lipid vesicles can be triggered by the peptide sequence ‘B18’ from the fertilization protein ‘bindin’, but it only proceeds efficiently in the presence of Zn^{2+} ions. We studied (i) the interaction of Zn^{2+} with the fusogenic peptide B18, (ii) the binding of B18 to 1-palmitoyl-2-oleoylglycero-3-phosphocholine (POPC), and (iii) the ternary system POPC/B18/ Zn^{2+} . The complex formation of Zn^{2+} with the central histidine-rich motif of B18 appears to shift the secondary structure away from a β -sheet towards an α -helical conformation. Here we observe for the first time an essentially α -helical structure of the peptide when immersed in POPC bilayers which appears to represent its functional fusogenic state. Infrared linear dichroism suggests a peripheral, oblique insertion mode of B18, mediated by the hydrophobic patches along one side of the amphipathic peptide. Furthermore, the hydration level of the peptide is reduced, suggesting that the hydrophobic region of the bilayer is involved in the lipid/peptide interactions. The hydration capacity of the POPC/B18/ Zn^{2+} system is distinctly smaller than that of POPC/ Zn^{2+} without peptide. The accompanying decrease in the number of tightly bound water molecules per lipid can be interpreted as a reduction in the repulsive ‘hydration’ forces, which usually prevent the spontaneous fusion of lipid vesicles. Binding of the B18 peptide in the presence of Zn^{2+} effectively renders the membrane surface more hydrophobic, thus allowing fusion to proceed. © 2000 Elsevier Science B.V. All rights reserved.

Keywords: Amphipathic peptide; Divalent cation; Membrane fusion; Fertilization protein; Infrared linear dichroism

1. Introduction

The sea urchin sperm protein ‘bindin’ plays a key role in fertilization, as it mediates the species-specific gamete adhesion and presumably fusion with the egg membrane [1,2]. The central conserved part of the protein is relatively hydrophobic and appears to be responsible for its high affinity to lipid bilayers [3–5]. To understand the function of native sperm bindin

and to illuminate the general principles of other fusogenic proteins, it is necessary to describe their mode of binding and their destabilization of fusion-competent lipid bilayers. To this aim, we are initially focussing our attention on a short sequence of 18 residues, which represents the minimal membrane-binding and fusogenic motif of bindin [6–8]. Just like the parent protein, the ‘B18’ peptide fragment has been demonstrated to cause rapid fusion between uncharged vesicles of sphingomyelin/cholesterol [7], and it also interacts strongly with other synthetic lipid bilayers (Zschoernig et al., in preparation). Notably, the fusion activity of the peptide is strongly

* Corresponding author. Fax: +49-341-9715709;
E-mail: binder@rz.uni-leipzig.de

enhanced in the presence of Zn^{2+} , which is known to occur in stoichiometric amounts in the parent protein. This metal ion has been shown to form a specific complex with the histidine-rich motif HxxHH of B18. Membrane fusion assays can thus be conveniently triggered by the addition of Zn^{2+} , which appears to act as a folding aid by introducing a local peptide conformation resembling the native zinc-binding site of bindin. By nuclear magnetic resonance (NMR) and circular dichroism (CD) spectroscopy, we have recently found that B18 forms an amphipathic α -helix in the presence of Zn^{2+} , and similarly in membrane-mimicking environments such as 30% trifluoroethanol (TFE) or detergent micelles [7,8].

In an α -helical conformation, which appears to be a characteristic structure of most fusogenic peptides [9,10], B18 carries two clusters of hydrophobic side chains. With these patches oriented on one face of the helix, the peptide could favorably penetrate into a lipid membrane. However, relatively little is known about the molecular interactions between B18 and lipids, and about the role that Zn^{2+} plays in this step. Besides any general structural changes of the relevant molecular segments, it will be interesting to address the orientation of the peptide in the lipid environment. An oblique angle of immersion has been postulated as a general mechanism for peptide-induced fusion, on the basis of molecular modelling [11]. Hence, an experimentally refined picture of the B18 system promises to be of some general relevance, not only for the fertilization process but also for other fusogenic peptides which mediate for example the entry of enveloped viruses into host cells.

The general process of peptide-induced membrane fusion must involve a sequence of events, namely peptide-binding, vesicle aggregation, surface dehydration and membrane destabilization, before the final merging of the bilayers can proceed [9,12,13]. The hydration of the polar interfaces and the repulsive forces acting between them are known to be closely related to the ability of lipid bilayers to fuse [14]. Consequently, an investigation of the membrane system as a function of hydration is expected to yield direct information about the thermodynamics of fusion, about the phase behavior of the lipid, and about the interactions of divalent cations and B18

with the lipid headgroups. Recently, we have combined hydration/dehydration studies with infrared (IR) linear dichroism measurements to characterize the molecular architecture of lipid systems [15–17]. Polarized attenuated total internal reflection (ATR) IR spectroscopy is well-suited to obtain information about the insertion mode of peptides into lipid membranes [18–23]. Hence we studied the interaction of B18 with oriented multibilayer stacks of 1-palmitoyl-2-oleoylglycero-3-phosphocholine (POPC) in the presence and absence of Zn^{2+} by IR linear dichroism as a function of the relative humidity (RH).

According to White and Wimley [24], the strategy for studying the interaction of a small biologically active peptide with a lipid bilayer is to answer four questions: (1) what structure does the peptide adopt; (2) what is the transbilayer location of the peptide; (3) what is the energetic cost of getting there; and (4) what are the resulting effects on the bilayer structure? Additionally, in this particular B18 system, we need to consider the influence of Zn^{2+} on the molecular structure of the lipid and peptide, and on the hydration levels of each individual component and a mixture of both. The paper is organized as follows: first, the secondary structure of the peptide in the presence and absence of Zn^{2+} is described. Second, its interactions with POPC and its orientation in the lipid membrane are analyzed and discussed. Third, we compare the water adsorption and the lyotropic chain melting transition of the lipid in four systems: pure POPC, POPC/ Zn^{2+} , POPC/B18 and POPC/ Zn^{2+} /B18. The results were discussed in terms of fusogenic activity.

2. Materials and methods

2.1. Materials and preparation of lipid vesicles

Vesicles of POPC (Avanti Polar Lipids, Alabaster, USA) were prepared as follows. The lipid in a chloroform/methanol stock solution (1:3 v/v) was dried and re-suspended by vortexing in water (D_2O or H_2O) at a final lipid concentration of 2–3 mg/ml, followed by extrusion (Lipex extruder, Biomembranes, Vancouver, Canada) of the suspension through a polycarbonate Unipore membrane (100 nm pore size, Millipore).

The peptide B18 (LGLLLRHLRHHSNLLANI), representing amino acids 103–120 of the mature *Strongylocentrotus purpuratus* bindin sequence, was synthesized by standard Fmoc protocols, purified by reverse phase high performance liquid chromatography and checked by electrospray mass spectroscopy, as described earlier [7,8]. Trifluoroacetic acid (TFA), which was used in these procedures, is known to interfere with the data analysis, as the COO⁻ stretching vibration can absorb strongly in the amide I region at 1673 cm⁻¹ [18,22]. Therefore, TFA was removed on an ion exchange column (Amberlite IRA-410 resin, Merck, Darmstadt, Germany), and the depletion was confirmed by ¹⁹F-NMR in solution. Stock solutions of B18 were prepared by dissolving the peptide in water (10 mM, D₂O or H₂O). Sample solutions were prepared by mixing appropriate amounts of stock solutions of the lipid, of the peptide and/or of ZnCl₂ (dissolved in D₂O or H₂O, 10 mM) to yield nominal peptide to lipid ratios of $R_{P/L} \approx 0, 0.02$ and 0.2 (mol/mol), and Zn²⁺ to lipid ratios between $R_{Z/L} = 0$ and 3 (mol/mol). Before measurements, the sample solutions were stored overnight at $T \approx 4^\circ\text{C}$.

2.2. IR linear dichroism measurements

Samples were prepared by pipetting 100–200 μl of the sample solution on a ZnSe ATR crystal ($70 \times 10 \times 5$ mm³ trapezoid, face angle 45° , six active reflections) and evaporating the water under a stream of warm air. While drying, the material was spread uniformly over an area of $A_{\text{film}} \approx 40 \times 7$ mm² onto the crystal surface by gently stroking with the pipette tip. The amount of material corresponds to an average thickness of the dry film of $d_0 > 3$ μm , assuming a density of 1 g/cm³.

The ATR crystal was mounted into a commercial horizontal ATR holder (Graseby Specac, Kent, UK) that had been modified such as to realize a well-defined RH and temperature (T) within the sample chamber [15]. We used a flowing water thermostat (Julabo, Seelbach, Germany) and a moisture generator (HumiVar, Leipzig, Germany) to adjust RH (D₂O or H₂O) to any value between 5% and 95%, with an accuracy of $\pm 0.5\%$ at $T = 30^\circ\text{C}$. Polarized absorbance spectra, $A_{\parallel}(\nu)$ and $A_{\perp}(\nu)$ (128 scans, nominal resolution 2 cm⁻¹), were recorded by means

of a Bio-Rad FTS-60a Fourier transform IR spectrometer (Digilab, MA, USA) at two perpendicular polarizations of the IR beam, parallel (\parallel) and perpendicular (\perp) with respect to the plane of incidence.

Before starting the measurements, the lipid films were hydrated for 1 h at RH = 95% and subsequently dried at 5%. Then, RH was increased stepwise (hydration scan). Polarized spectra were recorded every 3% after allowing the sample to equilibrate for 10 min at each step. After reaching the maximum value of RH, the scan direction was reversed (dehydration scan). In the samples without ZnCl₂, no hysteresis effects were detected. In the presence of ZnCl₂, the formation of a complex between POPC and Zn²⁺ was observed in the first hydration scan only after reaching a humidity of RH > 60% [25]. In view of this hysteresis, we exclusively present the results of dehydration scans.

Although we used D₂O vapor in most measurements, some experiments were performed with H₂O to prove that the spectrum of adsorbed D₂O, and in particular its bending mode near (1200–1204) cm⁻¹, does not lead to a misinterpretation of the IR spectra.

2.3. Determination of the IR order parameter

The IR order parameter, S_{IR} , of an absorption band was calculated by means of

$$S_{\text{IR}} = \frac{R - K_1^\infty}{R + K_2^\infty} \text{ with } R \equiv \frac{A_{\parallel}}{A_{\perp}} \quad (1)$$

The polarized absorbances, A_{\parallel} and A_{\perp} , were evaluated from $A_{\parallel}(\nu)$ and $A_{\perp}(\nu)$ by integration after baseline correction. In some cases, the bands were separated using a global fitting technique [26]. In general, the ‘constants’ $K_1(\xi) \equiv (E_{z'}/E_{y'})^2 + (E_{x'}/E_{y'})^2$ and $K_2(\xi) \equiv 2(E_{z'}/E_{y'})^2 - (E_{x'}/E_{y'})^2$ depend on the Cartesian coordinates of the normalized electric field amplitude (z' and y' point normal to the ATR surface and to the plane of incidence, respectively). These components depend on the ratio of the thickness of the sample film over the wavelength of the light ($\xi \equiv d/\lambda$), on the angle of incidence ($\omega = 45^\circ$), and on the ratio of the refractive indices of the sample and the ATR crystal ($n_{21} = n_{\text{sample}}/n_{\text{ZnSe}} = 0.58$) [27]. We make use of the ‘thick’ film approximation ($K_1^\infty = 2$ and $K_2^\infty = 2.54$, [27]) which has been shown

to yield acceptable results for lipid films on a ZnSe crystal at $\xi \geq 0.2$ [26].

The peak positions and the center of gravity (COG) of the absorption bands were determined from the weighted sum spectrum $A(\nu) = A_{\parallel}(\nu) + K_2^{\infty} A_{\perp}(\nu)$ [17,26].

2.4. Determination of water adsorption isotherms by means of ATR-IR spectroscopy

The mol ratio water to lipid, $R_{W/L}$, was estimated directly from the ratio of the integrated absorbances of the O–H/O–D stretching band of water, $\nu_{13}(\text{H}_2\text{O})/\nu_{13}(\text{D}_2\text{O})$, and the C=O stretching band of the lipid, $\nu(\text{C}=\text{O})$, by means of

$$R_{W/L} = K \cdot \frac{A_W(\nu_{13})}{A_L(\nu(\text{C}=\text{O}))} \quad (2)$$

This approximation is confirmed by comparison with the POPC isotherms, which were measured both gravimetrically and by IR spectroscopy to yield the proportionality constant K [25]. The $\nu_{13}(\text{D}_2\text{O})$ band was integrated over the range 2700 cm^{-1} – 2100 cm^{-1} , and $\nu_{13}(\text{H}_2\text{O})$ over 3700 cm^{-1} – 3100 cm^{-1} . The $\nu(\text{C}=\text{O})$ band provides a suited internal standard to determine $R_{W/L}$, because its integrated intensity (1780 cm^{-1} – 1690 cm^{-1}) decreases roughly proportional to the dilution effect of water [25].

3. Results and discussion

3.1. The effect of Zn^{2+} on the secondary structure of B18

Fig. 1 shows the IR spectra of B18 which is spread onto an ATR crystal at variable RH (D_2O). The shape of the amide I band is characterized by an intense IR band at 1620 – 1630 cm^{-1} , and a weak component 1685 cm^{-1} . The doublet is characteristic of an antiparallel β -sheet conformation [28,29]. This observation is fully consistent with the tendency of B18 to self-associate into β -sheet amyloid fibrils, as known from X-ray diffraction and electron microscopy [8]. Besides the doublet, an underlying band centered around 1667 cm^{-1} in D_2O vapor is clearly discernible. This feature appears to originate from an unordered structure of the peptide, which has also

been observed by CD spectroscopy for B18 in aqueous solution before precipitation into fibril sets in [6–8]. This interpretation is supported by the observation that in some freshly prepared IR samples, the amide I band shows a single peak near 1667 cm^{-1} , which transforms into the contour shown in Fig. 1 after incubation of the sample for several hours at $\text{RH} > 80\%$. In addition, the two asparagine side chains of B18 are expected to absorb at 1648 cm^{-1} , i.e. at a position in between the two β -sheet component bands [18,30]. The amide I band of B18 shows essentially the same structure in H_2O atmosphere as in D_2O . Note that the underlying H_2O bending vibration near 1650 cm^{-1} enhances, however, the central part of the amide I band.

The amide I contour of B18 in the presence of ZnCl_2 ($R_{Z/P} \approx 6.5$) differs fundamentally from that of pure B18, as it shows a single maximum at $\sim 1646 \text{ cm}^{-1}$ (D_2O) or 1658 cm^{-1} (H_2O). It can be attributed to an α -helical peptide structure, which is again in good agreement with previous reports on this system. CD studies had shown that the peptide assumes a predominantly α -helical conformation in the presence of Zn^{2+} , and that the B18- Zn^{2+} complexes self-associate further into globular particles that are held together via Zn^{2+} bridges [6–8]. The two shoulders in the IR bands at 1585 cm^{-1} and 1609 cm^{-1} are probably due to the symmetric and antisymmetric C=N stretchings of the charged arginine residues (CN_3D_5^+), which are superimposed on the imidazole ring vibration of histidine [18,30]. This interpretation is supported by the disappearance of the shoulders in the B18 spectrum in H_2O vapor, because the C=N stretching band shifts upwards by 40 – 50 cm^{-1} after protonation [31]. At this position, however, these bands are hidden behind the strong amide I and $\delta(\text{H}_2\text{O})$ water bands.

With increasing RH, the peak of the amide I band of B18 is shifted to lower wavenumbers by $\sim 4 \text{ cm}^{-1}$, both in the absence and presence of Zn^{2+} . This trend indicates a slight strengthening of the hydrogen bonds in the peptide backbone due to the adsorption of water [22] (vide infra).

The IR transmission spectra of B18 (5 mM) dissolved in pure D_2O or $\text{D}_2\text{O} + \text{ZnCl}_2$ show a dominant peak at $1670 \pm 3 \text{ cm}^{-1}$ (data not shown). This feature has been assigned to a disordered structure (vide supra) in accordance with previous results which

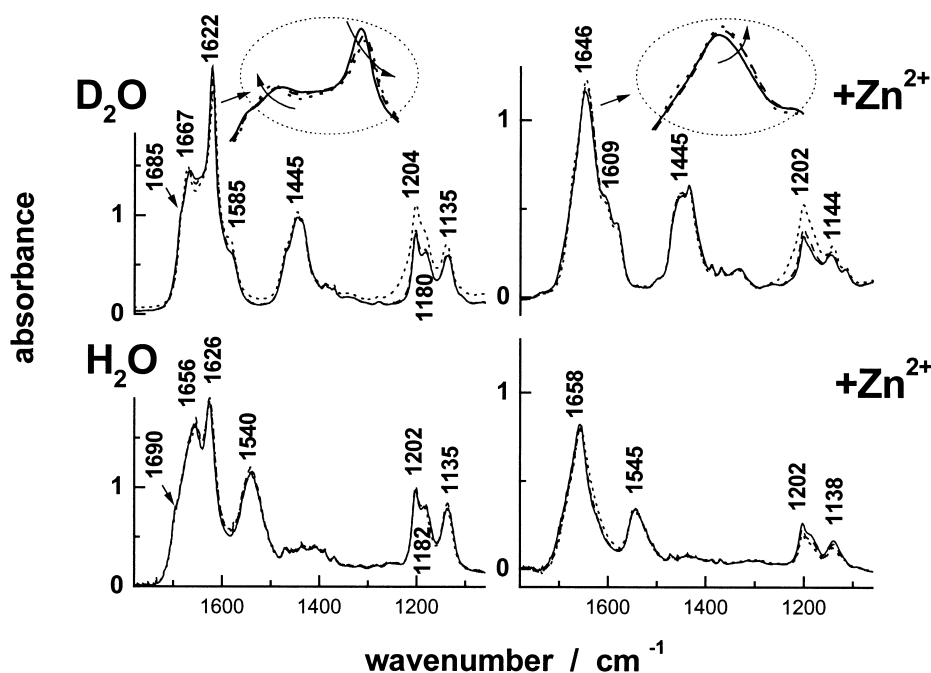


Fig. 1. IR spectra of B18 in the absence (left) and presence of Zn²⁺ (right) in a D₂O (above) and H₂O (below) atmosphere of RH = 8% (solid line), 59% (dotted) and 89% (dashed) at $T = 30^\circ\text{C}$. The insertions in the upper part enlarge the region of maximum intensity of the amide I band. The arrows indicate spectral shifts which are induced by hydration. Peak positions are given by vertical numbers in units of cm^{-1} . The intensity of the band at 1202 cm^{-1} (D₂O) increases at RH = 89% due to the underlying D₂O bending mode.

show that B18 is virtually unstructured in excess water up to pH 6 when the three histidines become protonated [7]. Precipitation of the peptide was observed in these samples only under neutral or basic conditions. Consequently, the existence of the β -sheet structure of the partially hydrated peptide indicates that at least a considerable fraction of the histidines must be deprotonated. The observed transformation of the peptide into an α -helical conformation at reduced hydration in the presence of Zn²⁺ confirms this interpretation, because the Zn²⁺ cations bind only to the deprotonated histidines [7]. Therefore we conclude that, even without having explicitly adjusted the pH (pD) in our preparation of the semi-dry B18/D₂O and B18/D₂O/ZnCl₂ mixtures, the histidines are sufficiently deprotonated to behave in a biologically relevant manner.

3.2. The secondary structure of membrane-bound B18

When the B18 peptide is added to POPC ($R_{P/L} = 0.02$), the amide I band is only weakly visible above the background of the dominant lipid IR spec-

trum (Fig. 2a). We have therefore subtracted the corresponding spectra of the systems without B18 from the polarized spectra of the membranes with B18, in order to filter out the amide I and II bands of the peptide (Fig. 2b,c; see legend of Fig. 2 for details). The contour of the amide I band suggests that B18 exhibits, at least partially, an α -helical conformation in both types of samples, i.e. with and without Zn²⁺. Apparently the lipid membrane induces an α -helical structure of the peptide even in the absence of Zn²⁺, despite the fact that B18 on its own tends to self-associate in a β -sheet conformation (vide supra). The assignment of the amide I band to a helical structure is still somewhat hypothetical, because a random conformation may give rise to a similar spectrum [32]. On the other hand, it is known from NMR spectroscopy that the peptide assumes a predominantly α -helical structure in detergent micelles and in 30% TFE [6,7]. Moreover, freeze-fracture electron microscopy has suggested that also in dimyristoylphosphatidylcholine (DMPC) bilayers, a certain fraction of α -helical peptide clusters is embedded, besides an abundance of

β -sheet fibrils which dominate the electron micrographs at high peptide concentration (lipid/peptide ratio = 10/1 or 30/1 (mol/mol), in the absence of Zn^{2+}) [8]. It seems that the tendency of B18 to self-associate into β -sheet fibrils is strongly concentration-dependent, since an α -helical structure is observed at the lower concentration limit used here (lipid/peptide ratio = 50/1). Indeed, we found at a 10-fold increased peptide concentration ($R_{P/L} = 0.2$), the IR amide I band of B18 in POPC retains the spectral features that are characteristic of a β -sheet (data not shown). Hence, the binding mode of B18 to uncharged membranes is strongly affected by peptide-peptide interactions, but at low concentration no significant amount of β -sheet structure was detected in the presence of POPC.

3.3. The orientation of membrane-bound B18

In view of the arguments presented above, it appears reasonable to assume a helical structure of the peptide when it is interacting with POPC. The mean orientation of this secondary structure with respect to the membrane surface can now be evaluated from the polarized IR difference spectra which are plotted in Fig. 2b,c. The $A_{\perp}(\nu)$ spectrum is multiplied by a factor $K_1^{\infty} = 2$ to take into account the differences in the relative power of the evanescent fields (vide supra). This representation shows that $2A_{\perp}(\nu) > A_{\parallel}(\nu)$ in the spectral range of the amide I band, which indicates that the mean angle $\langle \theta_{\mu} \rangle$, enclosed between the transition dipole, μ , and the normal of the ATR crystal, \mathbf{n} , is larger than 55° . Several factors have to be considered for a more detailed interpretation of the dichroism in terms of helix orientation. The IR order parameter can be expressed as a set of nested, uniaxial symmetric distributions [33]

$$S_{\text{IR}} = S_{\delta} S_{\theta} S_{\alpha}. \quad (3)$$

The order parameters S_{δ} , S_{θ} and S_{α} describe the mean macroscopic orientation of the membranes on the ATR surface (δ), the mean orientation of the molecular axis of the helix with respect to the bilayer (θ) and the mean orientation of the transition moment with respect to the helix axis (α) [17,26]. They are averaged second-order Legendre polynomials, $S_i \equiv 0.5 \langle 3\cos^2 i - 1 \rangle$ ($i = \delta, \theta, \alpha$), of the angles which

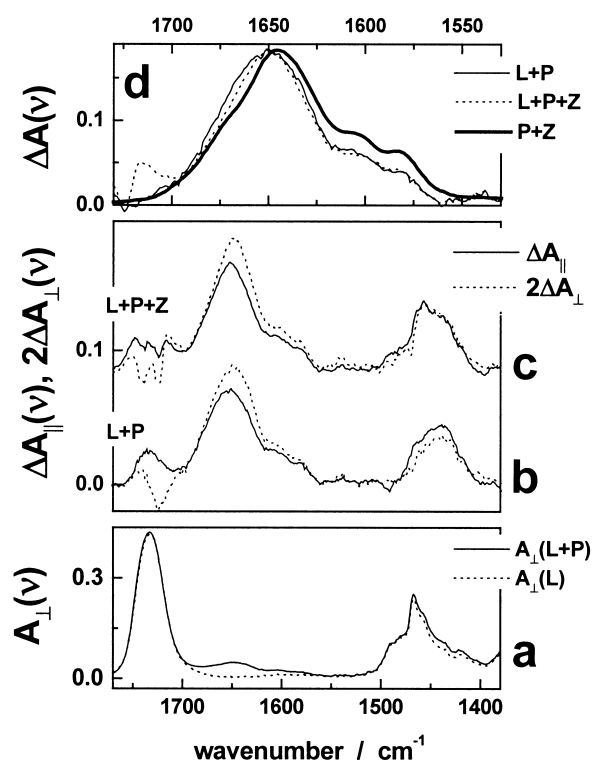


Fig. 2. Polarized IR spectra, $A_{\perp}(\nu)$, of POPC and of (POPC+B18) (a), the difference spectra $\Delta A_i = A_i(\text{L+P}) - k \cdot A_i(\text{L})$ ($i = \parallel, \perp$) in the absence (b) and presence (c) of Zn^{2+} , and the amide I region of the sum spectrum, $\Delta A = \Delta A_{\parallel} + K_2^{\infty} \cdot \Delta A_{\perp}$, of POPC+B18, POPC+B18+ Zn^{2+} and B18+ Zn^{2+} (d) at RH = 71% (D_2O) and $T = 30^{\circ}\text{C}$. The spectra are assigned in the figure. The correction factor, k , has been chosen to compensate the integral intensities of the $\nu(\text{C}=\text{O})$ band (1780 cm^{-1} – 1700 cm^{-1}) in the $A_{\perp}(\nu)$ spectrum, $A_{\perp}(\text{L+P}) - k \cdot A_{\perp}(\text{L}) = 0$. One value of k has been used to calculate $\Delta A_{\perp}(\nu)$ and $\Delta A_{\parallel}(\nu)$.

are enclosed between the local bilayer normal, \mathbf{d} , and \mathbf{n} (δ), between the helix axis, \mathbf{m} , and \mathbf{d} (θ), and between μ and \mathbf{m} (α). The macroscopic alignment of lipid lamellae of the ATR crystal yields typically $S_{\delta} \approx 1$, such that \mathbf{n} and \mathbf{d} can be assumed to point essentially parallel [34]. Literature data of $S_{\alpha}(\text{AI})$ vary between 0.4 and 0.8, which corresponds to an angle between μ and the helix axis, \mathbf{m} , of $40^{\circ} > \alpha(\text{AI}) > 20^{\circ}$ [20]. The intra-helical orientations reported for amide II transition dipoles vary between $\alpha(\text{AII}) = 90^{\circ}$ and 75° , or equivalently, $S_{\alpha}(\text{AII}) \approx -0.4$ to -0.5 .

The polarized spectra of POPC/B18 and POPC/B18/ Zn^{2+} yield virtually identical IR order parameters of the amide II band of $S_{\text{IR}}(\text{AII}) = 0.09 \pm 0.06$ and 0.0 ± 0.06 , respectively (RH = 71%). The order

parameter of the helix axis, $S_\theta \approx -0.1 \pm 0.15$, is calculated using Eq. 3 with $S_\alpha(\text{AII}) = -0.45$ ($\alpha(\text{AII}) \approx 79^\circ$) and $S_\delta = 1$. The analogous estimation for the amide I band using $S_{\text{IR}}(\text{AI}) = -0.09$ and $S_\alpha(\text{AI}) = 0.5$ ($\alpha(\text{AI}) \approx 35^\circ$) yields $S_\theta \approx -0.17 \pm 0.1$, in reasonable agreement with the result obtained from the dichroism of the amide II band.

The IR order parameter corresponds to an apparent mean inclination angle between the helix axes and the membrane normal of $\langle \theta \rangle \approx 60^\circ$. Two conclusions can be drawn from this estimation. First, there is no significant difference in helix orientation between the systems with and without Zn^{2+} . Second, the helix axis seems to align predominantly parallel to the membrane surface. One should, however, take into account several factors that prevent any exact analysis in terms of helix orientation: (i) as the individual amide transition dipoles are non-axially distributed with respect to the helix axis [21], a progressive summation along 10–20 residues (with a periodicity of 3.6 per turn) yields an uncertainty in S_{IR} of $\sim \pm 0.04$. (ii) A certain fraction of disordered peptide residues, for example at the helix-termini, would shift S_{IR} and S_θ towards a more random value. This effect would decrease the apparent inclination angle $\langle \theta \rangle$ of B18 towards 55° [19]. (iii) In the case of a kinked helical structure, the different orientations of the individual helical regions would lead to more complex averaging. The NMR structure of B18 in 30% TFE/ H_2O has indeed been found to consist of two helical parts that are connected via a flexible hinge in the histidine-rich center [7]. This loop is distinctly bent (90° – 120°) in the presence of detergent micelles, possibly due to their curved surface. Upon binding to a planar membrane surface, however, it has been suggested that the hinge may straighten out to form a stable α -helix over the full length of the peptide [7]. (iv) An equilibrium between membrane-bound monomers and oligomeric peptides would also complicate the IR analysis. Electron microscopy has revealed small B18 clusters of about 5 nm diameter embedded in DMPC (lipid/peptide ratio 30/1), although no such aggregates were observed in sphingomyelin/cholesterol under similar conditions [8]. (v) The dichroism of underlying absorption bands of amino acid side chains.

Most of these factors are expected to decrease the absolute value of the IR order parameter of the

amide bands towards the random value of 55° . Therefore, the apparent inclination angle, $\langle \theta \rangle$, should be judged as a lower limit rather than an overestimation of the in-plane alignment of the helix. Consequently, the experimental IR order parameter suggests that the helical axis of B18 is oriented nearly parallel, in a slightly oblique fashion with respect to the membrane surface. This picture is in good agreement with a recent functional model of fusogenic peptides, which have been proposed to act by penetrating no deeper than the ester linkages of the lipid into the target membrane at an oblique angle of the helix axis [9–11,35].

The amide I mode mainly represents a coupled peptide bond C=O stretching vibration. It is known to exhibit a remarkable red shift as the degree of hydration of the carbonyl oxygens increases [36,37]. The same tendency was observed upon hydration of B18, both on its own (see Section 3.2) as well as in the membrane-bound form (cf. Fig. 3). The amide I peak position of pure B18 is, however, considerably red-shifted relative to that in POPC (cf. Fig. 2d). This difference may suggest that membrane-bound B18 takes up less water than the ‘free’ peptide at a given RH. Indeed, if the peptide is partially buried within the membrane, some of the amide groups would be screened from the water. This interpretation is consistent with the slight disordering effect of the peptide on the lipid acyl chains (vide supra). Nevertheless, the differences in the amide I band positions may also be attributed to membrane-induced modifications of the peptide structure [29]. For example, a slight red shift of the amide I band of α -lactalbumin after the removal of Ca^{2+} ions has been reported to reflect a transition of the peptide from an α -helical into a more disordered, irregular structure [38]. This analogy would mean that pure B18 has a more disordered structure than the membrane-bound peptide. This interpretation, too, is consistent with the expected behavior of B18. In the presence of Zn^{2+} , no significant changes could be detected in the IR spectrum of membrane-bound B18. Only a slight narrowing of the amide I band may possibly indicate a more uniform secondary structure of the peptide in POPC with Zn^{2+} (Fig. 2d).

The spectrum of the dichroic ratio, $R(\nu)$, is virtually independent of RH and of Zn^{2+} in the amide I

region (Fig. 3, upper part). The variation of $R(\nu)$ across the band suggests that several populations of transition dipoles exist, being oriented more perpendicular relative to the membrane surface at $>1650\text{ cm}^{-1}$ and more perpendicular at smaller frequencies. A rough estimation, using the algorithm above with $S_{\text{IR}}(\text{left}) \approx -0.04 \pm 0.04$ and $S_{\text{IR}}(\text{right}) \approx -0.13 \pm 0.01$, yields $S_{\theta}(\text{left}) \approx -0.07 \pm 0.07$ and $S_{\theta}(\text{right}) \approx -0.26 \pm 0.02$. This would be equivalent to $\langle \theta \rangle_{\text{left}} \approx (55\text{--}60)^{\circ}$ and $\langle \theta \rangle_{\text{right}} \approx (67\text{--}66)^{\circ}$, i.e. a difference between the mean orientations of the helix axes of about $\sim 10^{\circ}$. It must be stressed here that a similar frequency-dependent dichroism spectrum has been observed for the amide I band of other membrane-bound polypeptides [18]. It has been tentatively explained by several effects: (i) two populations of helices may exist with different insertion modes into the membrane [18]. For example, the amide I band of well-oriented transmembrane helices is assumed to appear at bigger wavenumbers when compared with free, non-oriented polypeptides. (ii) In the case of annexin V bound to supported bilayers, a mixture of α -helical and β -sheet structures has been suggested to give rise to a more out of plane transition moment ($S_{\text{IR}} = 0.18$) for the high frequency component and a more in-plane transition moment ($S_{\text{IR}} = -0.11$) for the lower frequency component of the amide I band [39]. (iii) Alternatively, the amide I band could be split into two differently polarized subbands [18]. Simulations reveal that the amide I band of an α -helix can be decomposed into A-mode-like and E-mode-like subbands in the $1650\text{--}1660\text{ cm}^{-1}$ and $1620\text{--}1640\text{ cm}^{-1}$ regions, respectively [40].

Note that the spectrum of the dichroic ratio, $R(\nu)$, remains virtually unchanged in the region of the amide I band of B18 with increasing RH, even though the band position is considerably shifted towards smaller frequencies. Consequently, the mean order parameter of the amide I band decreases upon hydration from $S_{\text{IR}} \approx -0.06$ to -0.11 (the arrow in Fig. 3 illustrates the corresponding change of the dichroic ratio). This change would be equivalent to an increasing fraction of ‘in-plane’ helices, in terms of one of the models discussed above. Alternatively, one may suggest that the binding of water molecules to the peptide, especially to its carbonyl groups, changes the angle α (between the helix axis

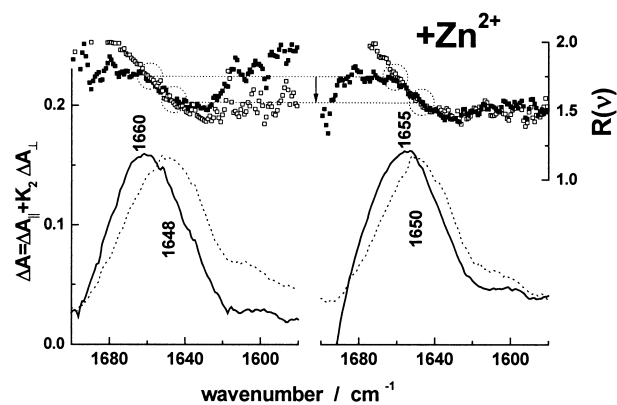


Fig. 3. Sum of the difference spectra, $\Delta A(\nu)$ (see legend of Fig. 2), of (POPC+B18) (left) and of (POPC+B18+ Zn^{2+}) (right) at RH = 5% (solid spectra) and 98% (dotted) at $T = 30^{\circ}\text{C}$. The corresponding spectra of the dichroic ratio are plotted above using solid and open squares for RH = 5% and 98%, respectively.

and the transition moment) and/or slightly modifies the secondary structure. A simple estimation by means of Eq. 3 suggests that the difference between the left and right flanks of $R(\nu)$ could be explained by a change of α from 20° to 45° at constant helix orientation. Despite these open questions, it is clear that the structure and orientation of membrane-bound B18 are practically the same in the gel phase and liquid-crystalline state of POPC, both in the presence and absence of Zn^{2+} .

3.4. Zn^{2+} -binding characteristics of POPC membranes

We demonstrated that zinc cations strongly interact with the polar groups of the zwitterionic lipid, and in particular with the negatively charged phosphate groups [25]. The formation of a 1:1 POPC: Zn^{2+} complex is paralleled by a conformational change of the C-O-P-O-C backbone from gauche/gauche into trans/trans. Furthermore, drastic dehydration of the lipids and metal cations is observed, both of which lose roughly 50% of their hydration shell. The energetic cost (on the scale of free enthalpy) for completely dehydrating the lipid headgroups is decreased by about 10 kJ/mol in the presence of Zn^{2+} . It appears that Zn^{2+} bridges between neighboring lipid molecules stabilize the gel phase relative to the liquid-crystalline state.

All studies with the peptide B18 and POPC in the presence of Zn^{2+} were performed at $R_{\text{Z/L}} \approx 0.7$ to

prevent the formation of free Zn^{2+} on the one hand, and to ensure that enough metal ions are available within the system on the other hand. The COG of the symmetric $\text{P}(\text{OC})_2$ stretching band near 765 cm^{-1} , $\text{COG}(v_s(\text{P}(\text{OC})_2))$, was used as a measure for the amount of Zn^{2+} which is bound to the lipid [25]. In the presence of Zn^{2+} , $\text{COG}(v_s(\text{P}(\text{OC})_2))$ slightly shifts towards smaller wavenumbers after the addition of B18 (not shown). This response is attributed to the transfer of Zn^{2+} from the lipid to the peptide, because B18 has no significant effect on $v_s(\text{P}(\text{OC})_2)$ in the absence of Zn^{2+} ions. Note that a B18-induced transformation of lipid-bound Zn^{2+} into ‘free’ Zn^{2+} can be excluded, because otherwise the hydration capacity of the mixture would be expected to increase, in contradiction to our observations. By quantitative analysis based on the empirical relation of Zn^{2+} -binding to POPC, we suggest that less than 0.1 zinc ions are removed from each lipid molecule on average, or equivalently, each B18 molecule binds less than five Zn^{2+} ions.

3.5. The effect of B18 on the lyotropic chain melting transition of POPC

Fig. 4 shows the COG and the IR order parameter, S_{IR} , of the symmetric methylene stretching band, $v_s(\text{CH}_2)$, of four different samples that were progressively dehydrated by decreasing the RH of the D_2O vapor atmosphere. We studied the lipid (POPC) in the presence and absence of Zn^{2+} and/or B18. The sigmoidal decrease of both spectral parameters, $S_{\text{IR}}(v_s(\text{CH}_2))$ and $\text{COG}(v_s(\text{CH}_2))$, is typical for the lyotropic liquid-crystalline/gel phase transition [17]. The freezing of the acyl chains into a predominantly stretched all-*trans* conformation is evident from the existence of the CH_2 wagging band progression at small RH (not shown, see [25]).

The position and width of the phase transition can be well-characterized from the first derivative $\text{COG}' = \partial\text{COG}(v_s(\text{CH}_2))/\partial\text{RH}$. When a first-order transition of a two-component mixture (water+lipid) is induced by changing the chemical potential of water by means of a variable RH, the transition must proceed at a unique value of $\text{RH} = \text{RH}_m$ under isobaric–isothermal conditions [41]. The full width at half maximum (FWHM) of the COG' curve of the dehydration scan of pure POPC (FWHM-

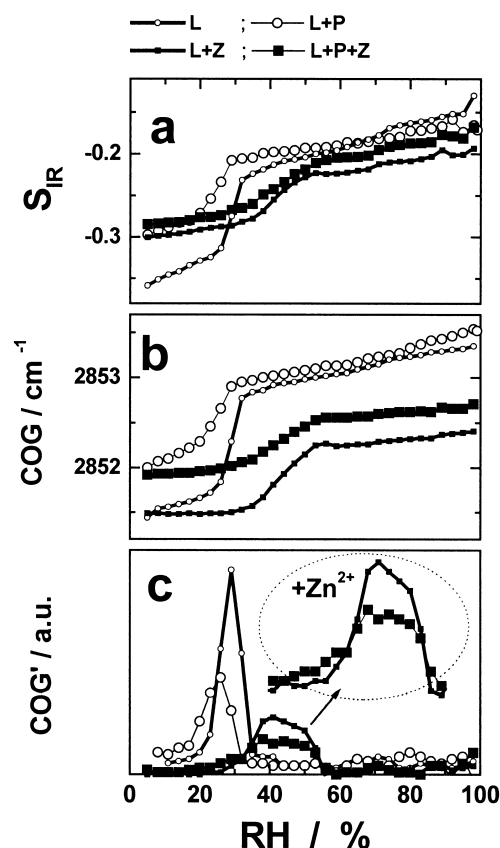


Fig. 4. IR order parameter, S_{IR} (a), COG (b), of the methylene stretching vibration and its first derivative, COG' (c), of POPC (L), POPC+ Zn^{2+} (L+Z, $R_{\text{Z}/\text{L}}=0.7$), POPC+B18 ($R_{\text{P}/\text{L}}=0.02$) and POPC+B18+ Zn^{2+} (L+P+Z, assignments of the symbols are given in the figure) as a function of the RH at $T=30^\circ\text{C}$. The COG' curves of the samples containing Zn^{2+} are enlarged in c.

(POPC) $\approx 8\%$) represents a kind of intrinsic width of the system, because it remains virtually the same at slower scan rates, when reversing the scan direction (hydration), or when changing the amount of material or its source of purchase (impurities). One may therefore suggest, for example, that several states of differently hydrated lipid molecules might be present, or that the coexistence of fluid and solid domains of microscopic size causes a certain broadening of the transition (vide infra). We will consider this question separately. Here the pure POPC will serve as a reference system for sake of comparison.

The addition of B18 ($R_{\text{P}/\text{L}}=0.02$) slightly shifts and widens the phase transition of POPC. These tendencies and the increased values of $S_{\text{IR}}(v_s(\text{CH}_2))$ (less negative at $\text{RH} < \text{RH}_m$) and of $\text{COG}(v_s(\text{CH}_2))$ indi-

cate that B18 probably decreases the molecular order within the hydrophobic core of the membranes, at least in the gel state, and thus destabilizes the solid phase of the lipid. Note that the COG of the methylene stretching band represents a qualitative measure of the conformational order of the hydrocarbon chains [42]. The gel phase disappears completely at a 10-fold increased amount of B18 ($R_{P/L}=0.2$, data not shown). Recent X-ray measurements showed that B18 perturbs the acyl chain packing of DMPC in the gel state, in agreement with our interpretation [8].

In contrast to B18, the presence of Zn^{2+} exerts the opposite effect on the phase transition ($R_{Z/L}=0.7$). The divalent ions stabilize the gel state of the lipid bilayer, because the center of the transition is shifted to a higher value of RH by $\Delta RH \approx 15\%$. The IR parameters $S_{IR}(v_s(CH_2))$ and $COG(v_s(CH_2))$ suggest that the hydrophobic core in the L_α phase is more ordered in the presence of Zn^{2+} than compared with pure POPC. This tendency can be explained by the formation of Zn^{2+} bridges, which connect the phosphate groups of adjacent lipids and thereby reduce the molecular area available to the acyl chains in the L_α phase [25].

The width of the lyotropic phase transition of POPC is found to be markedly increased in the presence of zinc, possibly due to a slightly different degree of Zn^{2+} -binding in the gel and L_α phases, and/or because of a microheterogeneous distribution of Zn^{2+} -lipid complexes and of free lipid. The phase transition of the system POPC+ Zn^{2+} +B18 remains essentially unchanged when compared with POPC+ Zn^{2+} , except for a slight broadening at the left hand flank of COG' . The interactions of the divalent cations with the lipid obviously represent the key factor that determines the phase behavior of the mixed system. The systematically bigger values of COG and S_{IR} indicate that the molecular order of the hydrocarbon chains is slightly decreased, probably due to peptide/lipid interactions.

3.6. The polar region of the membranes as a function of hydration

The continuous changes of the position of selected stretching bands of the carbonyl and phosphate groups of POPC with increasing RH are character-

istic signatures of the progressive hydration of the polar moieties. The presence of the peptide B18 has only a slight effect on the vibrational characteristics of the polar groups of the lipid, both in the absence and presence of Zn^{2+} (not shown). A small shift of the respective band positions after addition of B18 to POPC/ Zn^{2+} can be explained by the partial removal of Zn^{2+} from the lipid (vide supra). The IR order parameters of the absorption bands of the phosphate group in samples with and without Zn^{2+} do not change after the addition of B18. Hence, peptide-binding to the membrane clearly does not affect the mean orientation and conformation of the phosphate groups.

A slightly bigger (less negative) IR order parameter of the C=O stretching band of the carbonyl group in the presence of B18 can be interpreted in terms of a slight disordering effect of the peptide and/or of a smaller mean inclination angle of the C=O bonds with respect to the membrane normal.

3.7. Water-binding characteristics

The normalized IR absorption band of water in the different systems was transformed into an $R_{W/L}$ scale using Eq. 2. Fig. 5 shows that the lipid becomes considerably less hydrated in the presence of $ZnCl_2$.

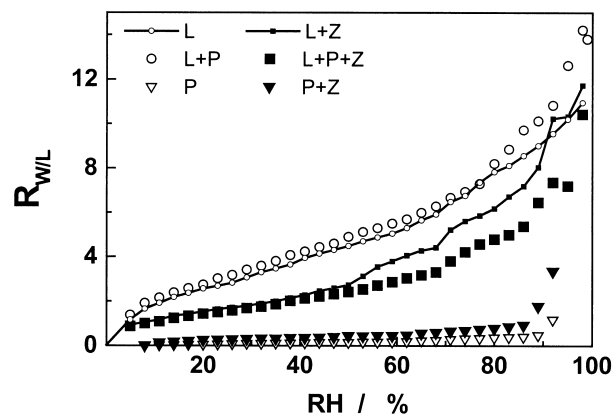


Fig. 5. Adsorption isotherms of POPC ('L', see figure for assignments of symbols), of B18 ('P') and of POPC+B18 ('L+P') in the presence and absence of $ZnCl_2$ ('Z'), as a function of RH ($R_{Z/L}=0.7$, $R_{P/L}=0.02$, $T=30^\circ C$). $R_{W/L}$ has been determined by means of IR (cf. Eq. 2). Maximum agreement between the gravimetric and IR isotherms was achieved when a constant amount of 0.8 water molecules per lipid was added to the gravimetric data. This correction can be explained by imperfect drying of the sample in the gravimetric experiment.

The peptide B18 per se, on the other hand, hardly affects the hydration of POPC, while the hydration of the mixture (POPC+B18+Zn²⁺) is further reduced below the level of the (POPC+Zn²⁺) system at the same RH. Hence, the water-binding capacity of the peptide and/or the lipid is significantly reduced in the presence of zinc.

Using the adsorption isotherms, it is possible to calculate the free enthalpy which drives the hydration process, according to [43,44]

$$G_{\text{dehyd}}(R_{\text{W/L}}) = RT \cdot \int_{a_{\text{w}}=1}^{a_{\text{w}}} \ln a_{\text{w}} \cdot dR_{\text{W/L}}(a_{\text{w}}) \quad (4)$$

The free enthalpy of dehydration, G_{dehyd} , represents a measure of the work to remove water from the fully hydrated system to a reduced water activity of $a_{\text{w}} = \text{RH}/100\% < 1$ [43]. G_{dehyd} can be fairly well-approximated over a wide range of $R_{\text{W/L}}$ by an exponential function, $G_{\text{dehyd}}(R_{\text{W/L}}) \approx G_{\text{dehyd}}^0 \cdot \exp(-R_{\text{W/L}}/R_{\text{W/L}}^0)$, which yields the free enthalpy of complete dehydration, G_{dehyd}^0 , and a characteristic number of ‘tightly bound’ water molecules, $R_{\text{W/L}}^0$ (cf. Fig. 6 and Table 1) [45]. The presence of Zn²⁺ reduces G_{dehyd}^0 by ~ 10 kJ/mol when compared with pure POPC and with POPC/B18.

The decay constant $R_{\text{W/L}}^0$ remains virtually unchanged when either metal ions or B18 alone are added to the lipid. On the other hand, $R_{\text{W/L}}^0$ decreases considerably in the presence of both additives, Zn²⁺ and B18. To illustrate the meaning of this result, let us assume a stack of lipid bilayers which are separated by water layers of thickness d_{W} . Then the number of lipid-bound water molecules can be represented on a geometric scale, using the relationship of $d_{\text{W}} \approx 2 \cdot v_{\text{W}} \cdot A_{\text{L}}^{-1} \cdot R_{\text{W/L}}$ (≈ 0.1 nm $\cdot R_{\text{W/L}}$). Here, it is assumed that the mean area requirement per lipid in the membrane plane and the volume per water molecule are roughly given by $A_{\text{L}} \approx 0.6$ nm² and $v_{\text{W}} \approx 0.03$ nm³, respectively [46]. The close approach and subsequent fusion of lipid bilayers in excess water requires a partial dehydration of the lipids in the region of contact. Hence, G_{dehyd} can be regarded as a measure of the energetic cost of pushing two bilayers together to a distance d_{W} , the thickness of the water gap between them. The thermal energy ($RT \approx 2.5$ kJ/mol at $T = 30^\circ\text{C}$) allows a spontaneous approach of the membranes

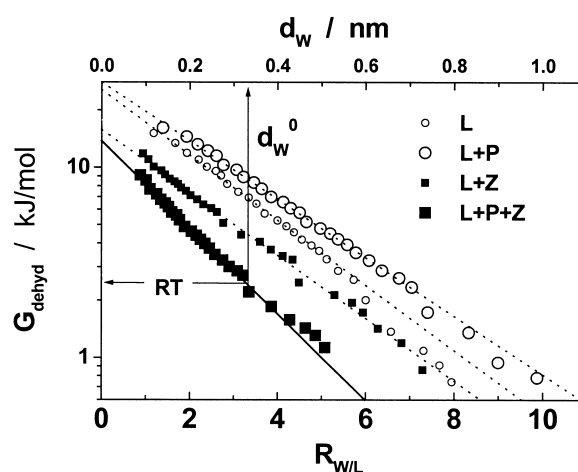


Fig. 6. Semilogarithmic plot of the free enthalpy of dehydration, G_{dehyd} , as a function of $R_{\text{W/L}}$. The lines are linear fits to obtain the slopes, $R_{\text{W/L}}^0$, and intercepts, G_{dehyd}^0 , which are summarized in Table 1. The arrows indicate $G_{\text{dehyd}} = RT$ ($T = 30^\circ\text{C}$) and the corresponding gap between opposite bilayers, d_{W}^0 , for L+P+Z (see text).

only within a certain d_{W} range that meets the condition $RT \geq G_{\text{dehyd}}$. An intrinsic ‘distance of closest approach’, d_{W}^0 , was estimated according to $RT = G_{\text{dehyd}}$ in the systems of interest (Table 1, see also Fig. 6). It typically adopts values that are bigger than the diameter of a water molecule (~ 0.4 nm). In these systems, at least a single layer of tightly bound water molecules prevents the direct contact between two apposing surfaces and thus the fusion of the lipid vesicles. In the presence of both B18 and Zn²⁺, d_{W}^0 is distinctly reduced. This increases the probability that thermal fluctuations can overcome the repulsion between the membranes such that fusion of the bilayers can occur. Indeed, whereas the peptide on its own only induces leakage of lipid

Table 1
Thermodynamic and structural data on the hydration of lipid/peptide/Zn²⁺ systems

System	G_{dehyd}^0 (kJ/mol)	$R_{\text{W/L}}^0$	d_{W}^0 (nm)
POPC	26	2.5	0.7
POPC+B18	28	2.8	0.6
POPC+Zn ²⁺	16	2.6	0.5
POPC+B18+Zn ²⁺	14	1.9	0.35

Standard errors: ± 2 kJ/mol (G_{dehyd}^0), ± 0.2 ($R_{\text{W/L}}^0$), ± 0.3 nm (d_{W}^0).

vesicles, the additional presence of Zn^{2+} has been demonstrated to trigger its fusogenic activity [6,7].

4. General aspects and summary

The main aim of this study was to characterize (i) the effect of Zn^{2+} on the secondary structure of the fusogenic peptide B18, (ii) to study the interaction of B18 with lipid membranes, and (iii) to analyze the corresponding Zn^{2+} -induced modifications. Our results can be summarized as follows.

1. Zinc ions govern the folding pathway of B18 in an aqueous environment, by shifting it away from a β -sheet structure and towards an α -helical conformation. The fusogenic activity of B18 has been attributed only to the latter, helical state [6,7]. It was suggested that the central histidine-rich motif, HxxHH, of B18 forms a Zn^{2+} complex via the two histidines in position i and $i+4$. This local loop could then act as a nucleation site for further folding into a more extended helix [7,47] (see Fig. 7 for illustration). It is known that the placement of histidine residues at positions i and $i+4$ of an α -helix mimics naturally occurring metal-binding sites of proteins [48,49].
2. POPC also induces an α -helical structure in the B18 peptide. A helical structure has been determined by NMR in membrane-mimicking environments, such as 30% TFE or detergent micelles [7]. Previous studies of B18 in lipid (in the absence of Zn^{2+}), on the other hand, had described a dominant self-association of the peptide into inactive β -sheet fibrils, presumably as a result of high peptide concentration. The formation of multimers at higher peptide/lipid ratios has been reported to occur in interaction studies of other fusogenic peptides with neutral phospholipids [9,10,50]. Here we observe for the first time an essentially α -helical structure of the peptide when immersed in uncharged POPC bilayers, which appears to represent its functional fusogenic state. Hence, the formation of an α -helix is triggered by a partially hydrophobic environment, which can stabilize the hydrophobic patches along one side of the amphipathic peptide (see Fig. 7 for illustration). Previous studies on other amphipathic peptides

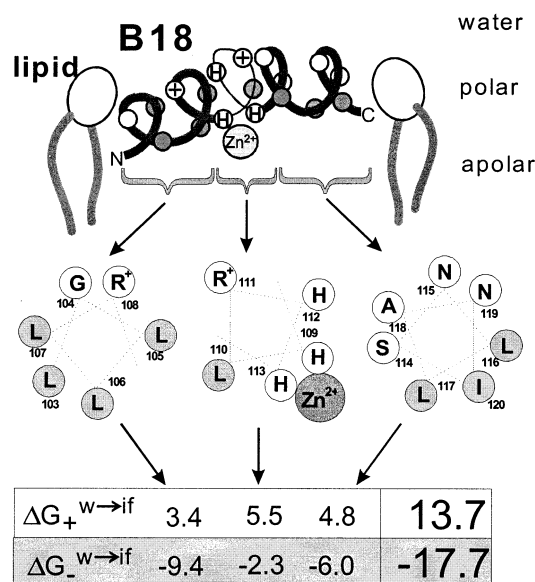


Fig. 7. Schematic representation of B18 in an α -helical structure which is induced by the binding of Zn^{2+} to the histidines (H) in the central part of the peptide (above). Hydrophobic and hydrophilic residues are indicated by gray and white circles, respectively. The position of the lipids illustrates a hypothetical insertion mode of B18 into a lipid membrane. The peptide is represented in terms of a helix-break-helix motif at the polar/apolar interface, where its hydrophobic and hydrophilic patches face the lipid and the water, respectively. The three parts of B18 are drawn in a helical wheel representation assuming a helix over the full length of B18 (middle, the residues are numbered according to the amino acids 103–120 of bindin from *S. purpuratus*). The table gives the sum of whole-residue free energies of transfer from water to POPC for the hydrophilic ($\Delta G_{+}^{w \rightarrow if} > 0$) and hydrophobic ($\Delta G_{-}^{w \rightarrow if} < 0$) residues, for the three parts of B18 and for the whole peptide (bold numbers, all data in kJ/mol) according to the single-residue data of [24].

have suggested that the interaction with a bilayer surface induces similar α -helical structures [11,51,52]. X-ray diffraction ([24] and references therein), fluorescence quenching measurements [35] and molecular dynamics simulations [53] have shown that many α -helical amphipathic peptides tend to align parallel to the membrane surface, within the polar/apolar boundary between the lipid headgroups and chains. Fusogenic peptides, in particular, appear to assume an oblique orientation.

A similar peripheral insertion mode of B18 is suggested here by the IR linear dichroism data. In good agreement with the postulated behavior, the fusogenic α -helix of B18 appears to enter the

membrane in a slightly oblique fashion. There are two hydrophobic patches on the same face of the B18 helix, which could be favorably embedded within the upper acyl chain region of the bilayer (Fig. 7). The sum of the whole-residue free energies of transfer from water to POPC, $\Delta G_{-}^{\text{w}\rightarrow\text{if}}$ and $\Delta G_{+}^{\text{w}\rightarrow\text{if}}$, yields a rough measure of the amphipathic nature of B18, and in particular of the preference for one side of the helix to immerse into the membrane (see table in Fig. 7) [24]. Note that these data refer to unfolded residues, and thus any simultaneous re-structuring into an α -helix is not considered. Despite this uncertainty, it becomes clear that the absolute value of $\Delta G_{-}^{\text{w}\rightarrow\text{if}}$ is comparable with that of G_{dehyd} . Hence, both processes, peptide–membrane interaction and lipid dehydration, compete at the same energetic scale. In the presence of Zn^{2+} , the gain of free enthalpy upon binding of the hydrophobic patch of B18 to the bilayer obviously overcompensates the costs of free enthalpy to dehydrate a few lipids partially. A slight modification of the IR order parameter of the lipid carbonyl C=O stretching band after binding of B18 seems to confirm the location of the peptide near the polar/apolar interface. The absence of any significant effects of B18 on the headgroup vibrations, however, indicates that there are no specific interactions between the peptide and the lipid headgroups. In particular, the stretching frequencies of the PO_2^- moieties, their mean orientation and hydration remain unaffected upon the binding of B18. There is apparently no preference of the charged arginines on the peptide to interact with the phosphate groups of POPC. Binding of the peptide to the membrane induces a shift in the lipid phase transition and decreases the molecular order of the acyl chains. Furthermore, the hydration level of the peptide is reduced, according to the position of the amide I band. These observations support our interpretation that the hydrophobic region of the bilayer is involved in the lipid/peptide interactions.

3. After addition of B18 to $\text{POPC}/\text{Zn}^{2+}$, a certain fraction of the metal ions is transferred from the lipid to the peptide. The IR characteristics of membrane-bound B18 are, however, virtually identical in the presence and absence of Zn^{2+} . Hence, the Zn^{2+} ions seem to interact with the

peptide, but without changing its structure and location to any significant extent. On the other hand, the hydration capacity of the $\text{POPC}/\text{B18}/\text{Zn}^{2+}$ system is distinctly smaller than that of $\text{POPC}/\text{Zn}^{2+}$. The accompanying decrease in the number of tightly bound water molecules per lipid can be interpreted as a reduction in the repulsive ‘hydration’ forces, which usually prevent the spontaneous fusion of lipid vesicles in dilute aqueous systems. Indeed, one of the motivations for this IR study was the observation that Zn^{2+} is necessary as a trigger for the histidine-rich peptide to fuse uncharged lipid bilayers. Hence, binding of the B18 peptide in the presence of Zn^{2+} effectively renders the membrane surface more hydrophobic and thus facilitates the contact between opposing bilayers before their final fusion.

Acknowledgements

This work was supported by the Deutsche Forschungsgemeinschaft within SFB 294 (TP C7) and SFB 197 (TP A10 and TP B13).

References

- [1] A. Hofmann, C.G. Glabe, *Semin. Dev. Biol.* 5 (1994) 233–242.
- [2] V.D. Vacquier, W.J. Swanson, M.E. Hellberg, *Dev. Growth Differ.* 37 (1995) 1–10.
- [3] L. Kennedy, P.L. DeAngelis, C.G. Glabe, *Biochemistry* 28 (1989) 9153–9158.
- [4] C.G. Glabe, *J. Cell. Biol.* 100 (1985) 794–799.
- [5] S.J. Miraglia, C.G. Glabe, *Biochim. Biophys. Acta* 1145 (1993) 191–198.
- [6] A. Ulrich, M. Otter, C.G. Glabe, D. Hoekstra, *J. Biol. Chem.* 273 (1998) 16748–16755.
- [7] R.W. Glaser, M. Grüne, C. Wandelt, A. Ulrich, *Biochemistry* 38 (1999) 2560–2569.
- [8] A.S. Ulrich, W. Tichelaar, G. Förster, O. Zschörnig, S. Weinkauff, H.W. Meyer, *Biophys. J.* 77 (1999) 829–841.
- [9] E.I. Pecheur, J. Sainte-Marie, A. Bievenue, D. Hoekstra, *J. Membr. Biol.* 167 (1999) 1–17.
- [10] S.R. Durell, I. Martin, J.-M. Ruyschaert, Y. Shai, R. Blumenthal, *Mol. Membr. Biol.* 14 (1997) 97–112.
- [11] R. Brasseur, T. Pillot, L. LIns, J. Vanderkerkhove, M. Rosseu, *Trends Biol. Sci.* 22 (1997) 169–171.
- [12] P.L. Yeagle, in: R.M. Epand (Ed.), *Current Topics in Mem-*

- branes, Vol. 44, Academic Press, San Diego, CA, 1998, pp. 375–401.
- [13] J. Zimmerberg, S.S. Vogel, L.V. Chernomordik, *Annu. Rev. Biophys. Biomol. Struct.* 22 (1993) 433–466.
- [14] K. Arnold, in: R. Lipowski and E. Sackmann (Eds.), *Handbook of Biological Physics*, Elsevier Science B.V., 1995, pp. 903–957.
- [15] H. Binder, A. Anikin, B. Kohlstrunk, G. Klose, *J. Phys. Chem. B* 101 (1997) 6618–6628.
- [16] H. Binder, T. Gutberlet, A. Anikin, G. Klose, *Biophys. J.* 74 (1998) 1908–1923.
- [17] H. Binder, A. Anikin, G. Lantzsch, G. Klose, *J. Phys. Chem. B* 103 (1999) 461–471.
- [18] E. Goormaghtigh, V. Raussens, J.-M. Ruyschaert, *Biochim. Biophys. Acta* 1422 (1999) 105–185.
- [19] B. Bechinger, J.-M. Ruyschaert, E. Goormaghtigh, *Biophys. J.* 76 (1999) 552–563.
- [20] E. Goormaghtigh, V. Cabiaux, J.M. Ruyschaert, *Subcell. Biochem.* 23 (1994) 329–362.
- [21] D. Marsh, *Biophys. J.* 75 (1998) 354–358.
- [22] P.I. Haris and D. Chapman, in: H.H.H. Mantsch and D. Chapman (Eds.), *Infrared Spectroscopy of Biomolecules*, Wiley and Sons, New York, 1996, pp. 239–278.
- [23] U.P. Fringeli, *Z. Nat.forsch. 32c* (1977) 20–45.
- [24] S.H. White, W.C. Wimley, *Biochim. Biophys. Acta* 1376 (1998) 339–352.
- [25] H. Binder, K. Arnold, A.S. Ulrich and O. Zschörnig, in preparation.
- [26] H. Binder, H. Schmiedel, *Vib. Spectrosc.* 21 (1999) 51–73.
- [27] N.J. Harrick, *Internal Reflection Spectroscopy*, Wiley, New York, 1967.
- [28] T. Miyazawa, *J. Chem. Phys.* 32 (1960) 1647–1652.
- [29] D.M. Byler, H. Susi, *Biopolymers* 25 (1986) 469–487.
- [30] Y.N. Chirgadze, O.V. Federov, N.P. Trushina, *Biopolymers* 14 (1975) 679–694.
- [31] S.Y. Venyaminov, N.N. Kalnin, *Biopolymers* 30 (1991) 1243–1257.
- [32] Y.N. Chirgadze, B.V. Shestopalov, S.Y. Venyaminov, *Biopolymers* 12 (1973) 1337–1351.
- [33] K.J. Rothschild, N.A. Clark, *Biophys. J.* 25 (1979) 473–488.
- [34] K.J. Rothschild, R. Sanches, T.L. Hsiao, N.A. Clark, *Biophys. J.* 31 (1980) 53–61.
- [35] A.H.A. Clayton, W.H. Sawyer, *Eur. Biophys. J.* 28 (1999) 133–141.
- [36] M. Kobayashi, M. Kobayashi, *J. Chem. Phys.* 84 (1980) 781–785.
- [37] E. Müller, A. Giehl, G. Schwarzmann, K. Sandhoff, A. Blume, *Biophys. J.* 71 (1996) 1400–1421.
- [38] S.J. Prestrelski, D.M. Byler, M.P. Thompson, *Biochemistry* 30 (1991) 8797–8804.
- [39] L. Silvestro, P.H. Axelsen, *Biochemistry* 38 (1999) 113–121.
- [40] H. Torii and M. Tasumi, in: H.H.H. Mantsch and D. Chapman (Eds.), *Infrared Spectroscopy of Biomolecules*, Wiley and Sons, New York, 1996, pp. 1–18.
- [41] H. Binder, B. Kohlstrunk, H.H. Heerklotz, *J. Coll. Interface Sci.* 220 (1999) 235–249.
- [42] V.R. Kodati, M. Lafleur, *Biophys. J.* 64 (1993) 163–170.
- [43] G. Cevc, in: E. Westhof (Ed.), *Water and Biological Macromolecules*, CRC Press, Boca Raton, FL, 1993, pp. 368–410.
- [44] A.S. Ulrich, A. Watts, *Biophys. Chem.* 49 (1994) 39–50.
- [45] R.P. Rand, V.A. Parsegian, *Biochim. Biophys. Acta* 988 (1989) 351–376.
- [46] G. Lantzsch, H. Binder, H. Heerklotz, M. Wendling, G. Klose, *Biophys. Chem.* 58 (1996) 289–302.
- [47] L. Regan, *Trends Biochem. Sci.* 20 (1995) 280–285.
- [48] D.W. Christianson, *Adv. Protein Chem.* 42 (1991) 281–355.
- [49] M.R. Ghadiri, C. Choi, *J. Am. Chem. Soc.* 112 (1990) 1630–1632.
- [50] C. Curtain, F. Separovic, K. Nielsen, D. Craik, Y. Zhong, A. Kirkpatrick, *Eur. Biophys. J.* 28 (1999) 427–436.
- [51] H. Vogel, *Biochemistry* 26 (1987) 4562–4572.
- [52] W.F. DeGrado, Z.R. Wasserman, J.D. Lear, *Science* 243 (1989) 622–628.
- [53] D.P. Tieleman, H.J.C. Berendsen, M.S.P. Sansom, *Biophys. J.* 76 (1999) 3186–3191.